

1 **The gut bacterial community potentiates *Clostridioides difficile***
2 **infection severity.**

3 **Running title:** Microbiota potentiates *Clostridioides difficile* infection severity

4 Nicholas A. Lesniak¹, Alyxandria M. Schubert¹, Kaitlyn J. Flynn¹, Jhansi L. Leslie^{1,4}, Hamide
5 Sinani¹, Ingrid L. Bergin³, Vincent B. Young^{1,2}, Patrick D. Schloss^{1,†}

6 † To whom correspondence should be addressed: pschloss@umich.edu

7 1. Department of Microbiology and Immunology, University of Michigan, Ann Arbor, MI

8 2. Division of Infectious Diseases, Department of Internal Medicine, University of Michigan
9 Medical School, Ann Arbor, MI

10 3. Unit for Laboratory Animal Medicine, University of Michigan, Ann Arbor, MI

11 4. Current affiliation: Department of Medicine, Division of International Health and

12 Infectious Diseases, University of Virginia School of Medicine, Charlottesville, Virginia, USA

13

14 **Abstract**

15 The severity of *Clostridioides difficile* infections (CDI) has increased over the last few
16 decades. Patient age, white blood cell count, creatinine levels as well as *C. difficile* ribotype
17 and toxin genes have been associated with disease severity. However, it is unclear whether
18 specific members of the gut microbiota associate with variation in disease severity. The gut
19 microbiota is known to interact with *C. difficile* during infection. Perturbations to the gut
20 microbiota are necessary for *C. difficile* to colonize the gut. The gut microbiota can inhibit *C.*
21 *difficile* colonization through bile acid metabolism, nutrient consumption and bacteriocin
22 production. Here we sought to demonstrate that members of the gut bacterial communities
23 can also contribute to disease severity. We derived diverse gut communities by colonizing
24 germ-free mice with different human fecal communities. The mice were then infected with
25 a single *C. difficile* ribotype 027 clinical isolate which resulted in moribundity and
26 histopathologic differences. The variation in severity was associated with the human fecal
27 community that the mice received. Generally, bacterial populations with pathogenic
28 potential, such as *Enterococcus*, *Helicobacter*, and *Klebsiella*, were associated with more
29 severe outcomes. Bacterial groups associated with fiber degradation, and bile acid
30 metabolism, such as *Anaerotignum*, *Blautia*, *Lactonifactor*, and *Monoglobus*, were associated
31 with less severe outcomes. These data indicate that, in addition to the host and *C. difficile*
32 subtype, populations of gut bacteria can influence CDI disease severity.

33 **Importance**

34 *Clostridioides difficile* colonization can be asymptomatic or develop into an infection,
35 ranging in severity from mild diarrhea to toxic megacolon, sepsis, and death. Models that

Deleted: there is an association between

Deleted: and

Deleted: *Escherichia*

Deleted: ,

Deleted: and lantibiotic production

Deleted: *Anaerostipes*

Deleted: *Coprobacillus*

43 predict severity and guide treatment decisions are based on clinical factors and *C. difficile*
44 characteristics. Although the gut microbiome plays a role in protecting against CDI, its
45 effect on CDI disease severity is unclear and has not been incorporated into disease
46 severity models. We demonstrated that variation in the microbiome of mice colonized with
47 human feces yielded a range of disease outcomes. These results revealed groups of bacteria
48 associated with both severe and mild *C. difficile* infection outcomes. Gut bacterial
49 community data from patients with CDI could improve our ability to identify patients at
50 risk of developing more severe disease and improve interventions which target *C. difficile*
51 and the gut bacteria to reduce host damage.

52

53 **Introduction**

54 *Clostridioides difficile* infections (CDI) have increased in incidence and severity since *C.*
55 *difficile* was first identified as the cause of antibiotic-associated pseudomembranous colitis
56 (1). CDI disease severity can range from mild diarrhea to toxic megacolon and death. The
57 Infectious Diseases Society of America (IDSA) and Society for Healthcare Epidemiology of
58 America (SHEA) guidelines define severe CDI in terms of a white blood cell count greater
59 than 15,000 cells/mm³ and/or a serum creatinine greater than 1.5 mg/dL. Patients who
60 develop shock or hypotension, ileus, or toxic megacolon are considered to have fulminant
61 CDI (2). Since these measures are CDI outcomes, they have limited ability to predict risk of
62 severe CDI when the infection is first detected. Schemes have been developed to score a
63 patient's risk for severe CDI outcomes based on clinical factors but have not been robust for
64 broad application (3). Thus, we have limited ability to prevent patients from developing
65 severe CDI.

66 Missing from CDI severity prediction models are the effects of the indigenous gut bacteria.
67 *C. difficile* interacts with the gut community in many ways. The indigenous bacteria of a
68 healthy intestinal community prevent *C. difficile* from infecting the gut (4). A range of
69 mechanisms can disrupt this inhibition, including antibiotics, medications, or dietary
70 changes, and lead to increased susceptibility to CDI (5–7). Once *C. difficile* overcomes the
71 inhibition and colonizes the intestine, the indigenous bacteria can either promote or inhibit
72 *C. difficile* through producing molecules or modifying the environment (8,9). Bile acids
73 metabolized by the gut bacteria can inhibit *C. difficile* growth and affect toxin production (4,
74 10,11). Bacteria in the gut also can compete more directly with *C. difficile* through

Deleted: provide a protective barrier preventing

Deleted: .

Deleted: barrier

Deleted: 4–6

Deleted: protective barrier

Deleted: 7,

Deleted: 9

82 antibiotic production or nutrient consumption (12–14). While the relationship between the
83 gut bacteria and *C. difficile* has been established, the effect the gut bacteria can have on CDI
84 disease severity is unclear.

Deleted: 11–13

85 Recent studies have demonstrated that when mice with diverse microbial communities
86 were challenged with a high-toxigenic strain resulted in varied disease severity (15) and
87 when challenged with a low-toxigenic strain members of the gut microbial community
88 associated with variation in colonization (16). Here, we sought to further elucidate the
89 relationship between members of the gut bacterial community and CDI disease severity
90 when challenged with a high-toxigenic strain, *C. difficile* ribotype 027 (RT027). We
91 hypothesized that since specific groups of gut bacteria affect the metabolism of *C. difficile*
92 and its clearance rate, specific groups of bacteria associate with variation in CDI disease
93 severity. To test this hypothesis, we colonized germ-free C57BL/6 mice with human fecal
94 samples to create varied gut communities. We then challenged the mice with *C. difficile*
95 RT027 and followed the mice for the development of severe outcomes of moribundity and
96 histopathologic cecal tissue damage. Since the murine host and *C. difficile* isolate were the
97 same and only the gut community varied, the variation in disease severity we observed was
98 attributable to the gut microbiome.

Deleted: 14

Deleted: 15

Deleted: infection dynamics, we can also identify
Deleted: that affect the
Deleted: of the infection

99 Results

100 ***C. difficile* is able to infect germ-free mice colonized with human fecal microbial
101 communities without antibiotics.** To produce gut microbiomes with greater variation
102 than those found in conventional mouse colonies, we colonized germ-free mice with
103 bacteria from human feces (17). We inoculated germ-free C57BL/6 mice with homogenized

Deleted: 16

111 feces from each of 15 human fecal samples via oral gavage. These human fecal samples
112 were selected because they represented diverse community structures based on
113 community clustering (18). After the gut communities had colonized for two weeks, we
114 confirmed them to be *C. difficile* negative by culture (19). We then surveyed the bacterial
115 members of the gut communities by 16S rRNA gene sequencing of murine fecal pellets
116 (Figure 1A). The bacterial communities from each mouse grouped more closely to those
117 communities from mice that received the same human fecal donor community than to the
118 mice who received a different human fecal donor community (Figure 1B). The communities
119 were primarily composed of populations of *Clostridia*, *Bacteroidia*, *Erysipelotrichia*, *Bacilli*,
120 and *Gammaproteobacteria*. However, the gut bacterial communities of each donor group of
121 mice harbored unique relative abundance distributions of the shared bacterial classes.

Deleted: 17) The
Deleted: were allowed to equilibrate
Deleted: post-inoculation (18).

122 Next, we tested this set of mice with their human-derived gut microbial communities for
123 susceptibility to *C. difficile* infection. A typical mouse model of CDI requires pre-treatment
124 of conventional mice with antibiotics, such as clindamycin, to become susceptible to *C.*
125 *difficile* colonization (20, 21). However, we wanted to avoid modifying the gut communities
126 with an antibiotic to maintain their unique microbial compositions and ecological
127 relationships. Since some of these communities came from people at increased risk of CDI,
128 such as recent hospitalization or antibiotic use (18), we tested whether *C. difficile* was able
129 to infect these mice without an antibiotic perturbation. We hypothesized that *C. difficile*
130 would be able to colonize the mice who received their gut communities from a donor with a
131 perturbed community. Mice were challenged with 10^3 *C. difficile* RT027 clinical isolate
132 spores. The mice were followed for 10 days post-challenge, and their stool was collected
133 and plated for *C. difficile* colony forming units (CFU) to determine the extent of the

Deleted: 19,
Deleted: 17

139 infection. Surprisingly, communities from all donors were able to be colonized (Figure 2).
140 Two mice were able to resist *C. difficile* colonization, both received their community donor
141 N1, which may be attributed to experimental variation since this group also had more mice.
142 By colonizing germ-free mice with different human fecal communities, we were able to
143 generate diverse gut communities in mice, which were susceptible to *C. difficile* infection
144 without further modification of the gut community.

145 **Infection severity varies by initial community.** After we challenged the mice with *C.*
146 *difficile*, we investigated the outcome from the infection and its relationship to the initial
147 community. We followed the mice for 10 days post-challenge for colonization density, toxin
148 production, and mortality. Seven mice, from Donors N1, N3, N4, and N5, were not colonized
149 at detectable levels on the day after *C. difficile* challenge but were infected ($>10^6$) by the
150 end of the experiment. All mice that received their community from Donor M1 through M6
151 succumbed to the infection and became moribund within 3 days post-challenge. The
152 remaining mice, except the uninfected Donor N1 mice, maintained *C. difficile* infection
153 through the end of the experiment (Figure 2). At 10 days post-challenge, or earlier for the
154 moribund mice, mice were euthanised and fecal material were assayed for toxin activity
155 and cecal tissue was collected and scored for histopathologic signs of disease (Figure 3).

156 Overall, there was greater toxin activity detected in the stool of the moribund mice (Figure
157 S1). However, when looking at each group of mice, we observed a range in toxin activity for
158 both the moribund and non-moribund mice (Figure 3A). Non-moribund mice from Donors
159 N2 and N5 through N9 had comparable toxin activity as the moribund mice, at 2 days post-
160 challenge. Additionally, not all moribund mice had toxin activity detected in their stool.

161 Next, we examined the cecal tissue for histopathologic damage. Moribund mice had high

Deleted: $P = 0.003$

Deleted: .

164 levels of epithelial damage, tissue edema, and inflammation (Figure S2) similar to
165 previously reported histopathologic findings for *C. difficile* RT027 (22). As observed with
166 toxin activity, the moribund mice had higher histopathologic scores than the non-moribund
167 mice ($P < 0.001$). However, unlike the toxin activity, all moribund mice had consistently
168 high histopathologic summary scores (Figure 3B). The non-moribund mice, Donor groups
169 N1 through N9, had a range in tissue damage from none detected to similar levels as the
170 moribund mice, which grouped by community donor. Together, the toxin activity,
171 histopathologic score, and moribundity showed variation across the donor groups but
172 were largely consistent within each donor group.

173 **Microbial community members explain variation in CDI severity.** We next interrogated
174 the bacterial communities at the time of *C. difficile* challenge (day 0) for their relationship
175 to infection outcomes using linear discriminant analysis (LDA) effect size (LEfSe) analysis
176 to identify individual bacterial populations that could explain the variation in disease

177 severity. We split the mice into groups by severity level based on moribundity or 10 days
178 post infection (dpi) histopathologic score for non-moribund. This analysis revealed
179 bacterial operational taxonomic units (OTUs) that were significantly different at the time of
180 challenge by the disease severity (Figure 4A). OTUs associated with *Akkermansia*,
181 *Bacteroides*, *Clostridium sensu stricto*, and *Turicibacter* were detected at higher relative
182 abundances in the mice that became moribund. OTUs associated with *Anaerotignum*,
183 *Enterocloster*, and *Murimonas* were more abundant in the non-moribund mice that would
184 develop only low intestinal injury. To understand the role of toxin activity in disease
185 severity, we applied LEfSe to identify the OTUs at the time of challenge that most likely
186 explain the differences between communities that had toxin activity detected at anytime

Deleted: S1

Deleted: 21

Deleted: their

Deleted: and

Deleted: We dichotomized the histopathologic scores into high and low groups by splitting on the median score of 5. ...

Deleted: 20 genera

Deleted: Bacterial genera *Turicibacter*, *Streptococcus*, *Staphylococcus*, *Pseudomonas*, *Phocaeicola*, *Parabacteroides*...

Deleted: and *Escherichia/Shigella*

Deleted: Populations of

Deleted: , *Coprobacillus*

Deleted: genera

Deleted: to

Deleted: the presence and absence of detected

204 point to those that did not (Figure 4B). An OTU associated with *Bacteroides*, OTU 7,
205 associated with the presence of toxin also associated with moribundity. Likewise, OTUs
206 associated with *Enterocloster* and *Murimonas* that were associated with no detected toxin,
207 also exhibited greater relative abundance in communities from non-moribund mice with a
208 low histopathologic score. Lastly, we tested for correlations between the endpoint (10 dpi)
209 relative abundances of OTUs and the histopathologic summary score (Figure 4C). The
210 endpoint relative abundance of *Bacteroides*, OTU 17, was positively correlated with
211 histopathologic score, as its day 0 relative abundance did with disease severity (Figure 4A).

212 A population of *Bacteroides*, OTU 17, was positively correlated with the histopathologic
213 score and were increased in the group of mice with detectable toxin. We also tested for
214 correlations between the endpoint relative abundances of OTUs and toxin activity but none
215 were significant. This analysis identified bacterial populations that were associated with
216 the variation in moribundity, histopathologic score, and toxin.

217 We next determined whether, collectively, bacterial community membership and relative
218 abundance could be predictive of the CDI disease outcome. We trained logistic regression
219 models with bacterial community relative abundance data from the day of colonization at
220 each taxonomic rank to predict toxin, moribundity, and histopathologic summary score.
221 For predicting if detectable toxin would be produced, microbial populations aggregated by
222 genus rank classification performed similarly as models using lower taxonomic ranks
223 (mean AUROC = 0.787, Figure S3). *C. difficile* increased odds of producing detectable toxin
224 when the community infected had less abundant populations of *Monoglobus*, *Akkermansia*,
225 *Extibacter*, *Intestinimonas* and *Holdemania* and had more abundant populations of
226 *Lachnospiraceae* (Figure 5A). Next, we assessed the ability of the community to predict

Deleted: Many genera that
Deleted: were
Deleted: , such as populations of *Escherichia/Shigella* and *Bacteroides*.
Deleted: there were genera such as *Anaerotignum*,
Deleted: ,
Deleted: that
Deleted: bacterial operational taxonomic units ()
Deleted:
Deleted: Populations of *Klebsiella* and *Prevotellaceae* were...
Deleted: genera
Deleted: random forest
Deleted: day 10 post-challenge
Deleted: phylum
Deleted: 83
Deleted: S2
Deleted: was more likely to produce
Deleted: *Verrucomicrobia*
Deleted: *Campilobacterota*
Deleted: *Proteobacteria*

248 moribundity. Bacteria grouped by order rank classification was sufficient to predict which
249 mice would succumb to the infection before the end of the experiment (mean AUROC =
250 0.9205, Figure S3). Many populations contributed to an increase odds of moribundity
251 (Figure 5B). Populations related to *Bifidobacteriales* and *Clostridia* decreased the odds of a
252 moribund outcome. Lastly, the relative abundances of OTUs were able to predict a high or
253 low histopathologic score 10 dpi (histopathologic scores were dichotomized as in previous
254 analysis, mean AUROC = 0.99, Figure S3). The model identified some similar OTUs as the
255 LEfSe analysis, such as *Murimonas* (OTU 48), *Bacteroides* (OTU 7), and *Hungatella* (OTU
256 24). These models have shown that the relative abundance of bacterial populations and
257 their relationship to each other could be used to predict the variation in moribundity,
258 histopathologic score, and detectable toxin of CDI.

259 **Discussion**

260 Challenging mice colonized with different human fecal communities with *C. difficile* RT027
261 demonstrated that variation in members of the gut microbiome affects *C. difficile* infection
262 disease severity. Our analysis revealed an association between the relative abundance of
263 bacterial community members and disease severity. Previous studies investigating the
264 severity of CDI disease involving the microbiome have had limited ability to interrogate
265 this relationship between the microbiome and disease severity. Studies that have used
266 clinical data have limited ability to control variation in the host, microbiome or *C. difficile*
267 ribotype (23). Murine experiments typically use a single mouse colony and different *C.*
268 *difficile* ribotypes to create severity differences (24). Recently, our group has begun
269 uncovering the effect microbiome variation has on *C. difficile* infection. We showed the

Deleted: class

Deleted: 91

Deleted: S2). The features with the greatest effect showed that communities with greater

Deleted: of bacteria belonging

Deleted: *Bacilli* and *Firmicutes* and reduced populations of *Erysipelotrichia* were more likely to result in

Deleted: Only one other class of bacteria was

Deleted: in

Deleted: mice, a group of unclassified *Clostridia*.

Deleted: genera

Deleted: S2). No genera had a significantly greater effect on the ...

Deleted: performance than any others, indicating the model was reliant on many genera for the correct prediction. The model used some of the genera

Deleted: in

Deleted: *Coprobacillus*, *Anaerostipes*,

Deleted: Communities with greater abundances of *Hungatella*, *Eggerthella*, *Bifidobacterium*, *Duncaniella* and *Neisseria* were more likely to have high histopathologic scores....

Deleted: 22

Deleted: 23

294 variation in the bacterial communities between mice from different mouse colonies
295 resulted in different clearance rates of *C. difficile* (16). We also showed varied ability of
296 mice to spontaneously eliminate *C. difficile* infection when they were treated with different
297 antibiotics prior to *C. difficile* challenge (25). Overall, the results presented here have
298 demonstrated that the gut bacterial community contributed to the severity of *C. difficile*
299 infection.

300 *C. difficile* can lead to asymptomatic colonization or infections with severity ranging from
301 mild diarrhea to death. Physicians use classification tools to identify patients most at risk of
302 developing a severe infection using white blood cell counts, serum albumin level, or serum
303 creatinine level (2, 26, 27). Those levels are driven by the activities in the intestine (28).
304 Research into the drivers of this variation have revealed factors that make *C. difficile* more
305 virulent. Strains are categorized for their virulence by the presence and production of the
306 toxins TcdA, TcdB, and binary toxin and the prevalence in outbreaks, such as ribotypes 027
307 and 078 (20, 29–32). However, other studies have shown that disease is not necessarily
308 linked with toxin production (33) or the strain (34). Furthermore, there is variation in the
309 genome, growth rate, sporulation, germination, and toxin production in different isolates of
310 a strain (35–38). This variation may help explain why severe CDI prediction tools often
311 miss identifying many patients with CDI that will develop severe disease (3, 24, 39, 40).
312 Therefore, it is necessary to gain a full understanding of all factors contributing to disease
313 variation to improve our ability to predict severity.

314 The state of the gut bacterial community determines the ability of *C. difficile* to colonize and
315 persist in the intestine. *C. difficile* is unable to colonize an unperturbed healthy murine gut

Deleted: 15

Deleted: 24

Deleted: 25,

Deleted: 27

Deleted: 19, 28–31

Deleted: 32

Deleted: 33

Deleted: 34–37

Deleted: 23, 38

325 community and is only able to become established after a perturbation (21). Once
326 colonized, the different communities lead to different metabolic responses and dynamics of
327 the *C. difficile* population (9, 25, 41). Gut bacteria metabolize primary bile acids into
328 secondary bile acids (4, 42, 43). The concentration of these bile acids affects germination,
329 growth, toxin production and biofilm formation (10, 11, 44, 45). Members of the bacterial
330 community also affect other metabolites *C. difficile* utilizes. *Bacteroides thetaiotaomicron*
331 produce sialidases which release sialic acid from the mucosa for *C. difficile* to utilize (46,
332 47). The nutrient environment affects toxin production (48). Thus, many of the actions of
333 the gut bacteria modulate *C. difficile* in ways that could affect the infection and resultant
334 disease.

335 A myriad of studies have explored the relationship between the microbiome and CDI
336 disease. Studies examining difference in disease often use different *C. difficile* strains or
337 ribotypes in mice with similar microbiota as a proxy for variation in disease, such as strain
338 630 for non-severe and RT027 for severe (20, 29, 30, 49). Studies have also demonstrated
339 variation in infection through tapering antibiotic dosage (21, 25, 50) or by reducing the
340 amount of *C. difficile* cells or spores used for the challenge (20, 50). These studies often
341 either lack variation in the initial microbiome or have variation in the *C. difficile* infection
342 itself, confounding any association between variation in severity and the microbiome.
343 Recent studies have shown variation in the initial microbiome, via different murine
344 colonies or colonizing germ-free mice with human feces, that were challenged with *C.*
345 *difficile* resulted in varied outcomes of the infection (15, 16, 51).

Deleted: 20

Deleted: 8, 24, 40

Deleted: 41

Deleted: 9,

Deleted: 43

Deleted: 45,

Deleted: 47

Deleted: 19, 28

Deleted: 48

Deleted: 20, 24, 49

Deleted: 19, 49

Deleted: 14,

358 Our data have demonstrated gut bacterial relative abundances associate with variation in
359 toxin production, histopathologic scoring of the cecal tissue and mortality. This analysis
360 revealed populations of *Akkermansia*, *Anaerotignum*, *Blautia*, *Enterocloster*, *Lactonifactor*,
361 and *Monoglobus* were more abundant in the microbiome of non-moribund mice which had
362 low histopathologic scores and no detected toxin. The protective role of these *bacteria* are
363 supported by previous studies. *Blautia*, *Lactonifactor*, and *Monoglobus* have been shown to
364 be involved in dietary fiber fermentation and associated with healthy communities (52–
365 54). *Anaerotignum*, which produce short chain fatty acids, *has* been associated with healthy
366 communities (55, 56). *Akkermansia* and *Enterocloster* were also identified as more
367 abundant in mice which had a low histopathologic scores but have contradictory
368 supporting evidence in the current literature. In our data, a population of *Akkermansia*,
369 *OTU 5*, was most abundant in the non-moribund mice with low histopathologic scores but
370 moribund mice had increased population of *Akkermansia*, *OTU 8*. This difference could
371 indicate either a more protective mucus layer was present inhibiting colonization (57, 58)
372 or mucus consumption by *Akkermansia* could have been crossfeeding *C. difficile* or exposing
373 a niche for *C. difficile* (59–61). Similarly, *Enterocloster* was more abundant and associated
374 with low histopathologic scores. It has been associated with healthy populations and has
375 been used to mono-colonize germ-free mice to reduce the ability of *C. difficile* to colonize
376 (62, 63). However, *Enterocloster* has also been involved in infections, such as bacteremia
377 (64, 65). These data have exemplified populations of bacteria that have the potential to be
378 either protective or harmful. Thus, the disease outcome is not likely based on the
379 abundance of individual populations of bacteria, rather it is the result of the interactions of
380 the community.

Deleted: *Anaerostipes*, *Coprobacillus*

Deleted: genera

Deleted: *Coprobacillus*

Deleted: 50–53). *Anaerostipes* and *Coprobacillus*

Deleted: have

Deleted: 54–

Deleted: Furthermore, *Coprobacillus*, which was abundant in mice with low histopathologic scores but rare in all other mice, has been shown to contain a putative type I lantibiotic gene cluster and inhibit *C. difficile* colonization (57–59).

Deleted: there were some

Deleted: which

Deleted: populations

Deleted: be attributed to

Deleted: 59, 60

Deleted: –63

Deleted: 64, 65

Deleted: 66, 67

400 The groups of bacteria that were associated with either a higher histopathologic score or
401 moribundity are members of the indigenous gut community that also have been associated
402 with disease, often referred to as opportunistic pathogens. Some of the populations of
403 *Bacteroides*, *Enterococcus*, and *Klebsiella* that associated with worse outcomes, have been
404 shown to have pathogenic potential, expand after antibiotic use, and are commonly
405 detected in CDI cases (66–69). In addition to these populations, *Eggerthella*, *Prevotellaceae*
406 and *Helicobacter*, which associated with worse outcomes, have also been associated with
407 intestinal inflammation (70–72). Recently, *Helicobacter hepaticus* was shown to be
408 sufficient to cause susceptibility to CDI in IL-10 deficient C57BL/6 mice (73). In our
409 experiments, when *Helicobacter* was present, the infection resulted in a high
410 histopathologic score (Figure 4C). While we did not use IL-10 deficient mice, it is possible
411 the bacterial community or host response are similarly modified by *Helicobacter*, allowing
412 *C. difficile* infection and host damage. These bacteria groups increased in severe outcomes
413 maintained their differences throughout the length of the experiment (Figure S4). These
414 results agreed Aside from *Helicobacter*, these groups of bacteria that associated with more
415 severe outcomes did not have a conserved association between their relative abundance
416 and the disease severity across all mice.

417 Since we observed groups of bacteria that were associated with less severe disease it may
418 be appropriate to apply the damage-response framework for microbial pathogenesis to CDI
419 (74, 75). This framework posits that disease is not driven by a single entity, rather it is an
420 emergent property of the responses of the host immune system, infecting microbe, *C.*
421 *difficile*, and the indigenous microbes at the site of infection. In the first set of experiments,
422 we used the same host background, C57BL/6 mice, the same infecting microbe, *C. difficile*

Deleted: Many

Deleted: with pathogenic potential

Deleted: are also facultative anaerobes. *Enterococcus*,
Klebsiella, *Shigella*/*Escherichia*, *Staphylococcus*, and
Streptococcus...

Deleted: (17, 68, 69)

Deleted: 70–73

Deleted: 74–76

Deleted: 77

Deleted: 78, 79

433 RT027 clinical isolate 431, with different gut bacterial communities. The bacterial groups
434 in those communities were often present in both moribund and non-moribund and across
435 the range of histopathologic scores. Thus, it was not merely the presence of the bacteria but
436 their activity in response to the other microbes and host which affect the extent of the host
437 damage. Additionally, while each mouse and *C. difficile* population had the same genetic
438 background, they too were reacting to the specific microbial community. Different gut
439 microbial communities can also have different effects on the host immune responses (76).
440 Disease severity is driven by the cumulative effect of the host immune response and the
441 activity of *C. difficile* and the gut bacteria. *C. difficile* drives host damage through the
442 production of toxin. The gut microbiota can modulate host damage through the balance of
443 metabolic and competitive interactions with *C. difficile*, such as bacteriocin production or
444 mucin degradation, and interactions with the host, such as host mucus glycosylation or
445 intestinal IL-33 expression (15, 77). For example, low levels of mucin degradation can
446 provide nutrients to other community members producing a diverse non-damaging
447 community (78). However, if mucin degradation becomes too great it reduces the
448 protective function of the mucin layer and exposes the epithelial cells. This over-harvesting
449 can contribute to the host damage due to other members producing toxin. Thus, the
450 resultant intestinal damage is the balance of all activities in the gut environment. Host
451 damage is the emergent property of numerous damage-response curves, such as one for
452 host immune response, one for *C. difficile* activity and another for microbiome community
453 activity, each of which are a composite curve of the individual activities from each group,
454 such as antibody production, neutrophil infiltration, toxin production, sporulation, fiber
455 and mucin degradation. Therefore, while we have identified populations of interest, it may

Deleted: 14, 80

Deleted: 81

458 be necessary to target multiple types of bacteria to reduce the community interactions
459 contributing to host damage.

460 Here we have shown several bacterial groups and their relative abundances associated
461 with variation in CDI disease severity. Further understanding how the microbiome affects
462 severity in patients could reduce the amount of adverse CDI outcomes. When a patient is
463 diagnosed with CDI, the gut community composition, in addition to the traditionally
464 obtained clinical information, may improve our severity prediction and guide prophylactic
465 treatment. Treating the microbiome at the time of diagnosis, in addition to *C. difficile*, may
466 prevent the infection from becoming more severe.

467 Materials and Methods

468 **Animal care.** 6- to 13-week old male and female germ-free C57BL/6 were obtained from a
469 single breeding colony in the University of Michigan Germ-free Mouse Core. Mice (M1 n=3,
470 M2 n=3, M3 n=3, M4 n=3, M5 n=7, M6 n=3, N1 n=11, N2 n=7, N3 n=3, N4 n=3, N5 n=3, N6
471 n=3, N7 n=7, N8 n=3, N9 n=2) were housed in cages of 2-4 mice per cage and maintained in
472 germ-free isolators at the University of Michigan germ-free facility. All mouse experiments
473 were approved by the University Committee on Use and Care of Animals at the University
474 of Michigan.

Deleted: , M1 n=3, M2 n=3, M3 n=3, M4 n=3, M5 n=7, M6 n=3...

475 ***C. difficile* experiments.** Human fecal samples were obtained as part of Schubert *et al.* and
476 selected based on community clusters (18) to result in diverse community structures.
477 (Table S1). Feces were homogenized by mixing 200 mg of sample with 5 ml of PBS. Mice
478 were inoculated with 100 μ l of the fecal homogenate via oral gavage. Two weeks after the
479 fecal community inoculation, mice were challenged with *C. difficile*. Stool samples from

Deleted: 17

Deleted: .

484 each mouse were collected one day prior to *C. difficile* and plated for *C. difficile* enumeration
485 to confirm no *C. difficile* was detected in stool prior to challenge. *C. difficile* clinical isolate
486 431 came from Carlson *et al.* which had previously been isolated and characterized (35, 36) Deleted: 34
487 and has recently been further characterized (37). Spores concentration were determined Deleted: 36
488 both before and after challenge (79). 10³ *C. difficile* spores were given to each mouse via Deleted: 82
489 oral gavage.

490 **Sample collection.** Fecal samples were collected on the day of *C. difficile* challenge and the
491 following 10 days. Each day, a fecal sample was collected and a portion was weighed for
492 plating (approximately 30 mg) and the remaining sample was frozen at -20°C.
493 Anaerobically, the weighed fecal samples were serially diluted in PBS, plated on TCCFA
494 plates, and incubated at 37°C for 24 hours. The plates were then counted for the number of
495 colony forming units (CFU) (80). Deleted: 83

496 **DNA sequencing.** From the frozen fecal samples, total bacterial DNA was extracted using
497 MOBIO PowerSoil-htp 96-well soil DNA isolation kit. We amplified the 16S rRNA gene V4
498 region and sequenced the resulting amplicons using an Illumina MiSeq as described
499 previously (81). Deleted: 84

500 **Sequence curation.** Sequences were processed with mothur(v.1.44.3) as previously
501 described (81, 82). In short, we used a 3% dissimilarity cutoff to group sequences into Deleted: 84, 85
502 operational taxonomic units (OTUs). We used a naive Bayesian classifier with the
503 Ribosomal Database Project training set (version 18) to assign taxonomic classifications to
504 each OTU (83). We sequenced a mock community of a known community composition and Deleted: 86

512 16s rRNA gene sequences. We processed this mock community with our samples to
513 calculate the error rate for our sequence curation, which was an error rate of 0.19%.

514 **Toxin cytotoxicity assay.** To prepare the sample for the activity assay, fecal material was
515 diluted 1:10 weight per volume using sterile PBS and then filter sterilized through a 0.22-
516 μ m filter. Toxin activity was assessed using a Vero cell rounding-based cytotoxicity assay as
517 described previously (30). The cytotoxicity titer was determined for each sample as the last
518 dilution, which resulted in at least 80% cell rounding. Toxin titers are reported as the log10
519 of the reciprocal of the cytotoxicity titer.

Deleted: 29

520 **Histopathology evaluation.** Mouse cecal tissue was placed in histopathology cassettes and
521 fixed in 10% formalin, then stored in 70% ethanol. McClinchey Histology Labs,
522 Inc. (Stockbridge, MI) embedded the samples in paraffin, sectioned, and created the
523 hematoxylin and eosin-stained slides. The slides were scored using previously described
524 criteria by a board-certified veterinary pathologist who was blinded to the experimental
525 groups (30). Slides were scored as 0-4 for parameters of epithelial damage, tissue edema,
526 and inflammation and a summary score of 0-12 was generated by summing the three

Deleted: 29

527 individual parameter scores. For non-moribund mice, histopathological summary scores
528 used for LEfSe and logistic regression were split into high and low groups based on greater
529 or less than the median summary score of 5 because the had a bimodal distribution ($P <$

530 0.05).

531 **Statistical analysis and modeling.** To compare community structures, we calculated Yue
532 and Clayton dissimilarity matrices (θ_{YC}) in mothur (84). For this calculation, we averaged of
533 1000 sub-samples, or rarified, samples to 2,107 sequence reads per sample to limit uneven

Deleted: 87). We rarefied

Deleted: sequences

538 sampling biases. We tested for differences in individual taxonomic groups that would
539 explain the outcome differences with LEfSe ([85](#)) in mothur (default parameters, LDA > 4).
540 We tested for differences in temporal trends through fitting a linear model to each OTU and
541 testing for differences between histopathological summary scores with LEfSe (85) in
542 mothur (default parameters, LDA > 3). Remaining statistical analysis and data visualization
543 was performed in R (v4.0.5) with the tidyverse package (v1.3.1). We tested for significant
544 differences in β -diversity (θ_{YC} , histopathological scores, and toxin activity using the
545 Wilcoxon rank sum test, non-unimodality to non-moribund histopathological summary
546 score using Hartigans' dip test, and toxin detection in mice using the Pearson's Chi-square
547 test. We used Spearman's correlation to identify which OTUs that had a correlation
548 between their relative abundance and the histopathologic summary score. P values were
549 then corrected for multiple comparisons with a Benjamini and Hochberg adjustment for a
550 type I error rate of 0.05 ([86](#)). We built L2 logistic regression models using the mikropml
551 package ([87](#)). Sequence counts were summed by taxonomic ranks from day 0 samples,
552 normalized by centering to the feature mean and scaling by the standard deviation, and
553 features positively or negatively correlated were collapsed into a single feature. For each
554 L2 logistic regression model, we ran 100 random iterations using values of 1e-0, 1e1, 1e2,
555 2e2, 3e2, 4e2, 5e2, 6e2, 7e2, 8e2, 9e2, 1e3, 1e4 for the L2 regularization penalty with a split
556 of 80% of the data for training and 20% of the data for testing. Lastly, we did not compare
557 murine communities to donor community or clinical data because germ-free mice
558 colonized with non-murine fecal communities have been shown to more closely resemble
559 the murine communities than the donor species community ([88](#)). Furthermore, it is not our

Deleted: 88) in mothur.

Deleted:) using the Wilcoxon rank sum test.

Deleted: 89

Deleted: random forest

Deleted: 90) with relative abundance

Deleted: using mtry values of 1 through 10, 15, 20, 25, 40, 50, 100. The split for training and testing varied

Deleted: model

Deleted: avoid overfitting

Deleted: data. To determine

Deleted: optimal split

Deleted: tested splits (50%, 60%, 70%, 80%, 90% data used for training) to find

Deleted: greatest portion

Deleted: data that could be used to train the model while still maintaining the same performance for the training model as the model with the held-out test data. The toxin and moribundity models were trained with 60

Deleted: . The histopathologic score model was trained with 80...

Deleted: 91

581 intention to make any inferences regarding human associated bacteria and their
582 relationship with human CDI outcome.

583 **Code availability.** Scripts necessary to reproduce our analysis and this paper are available
584 in an online repository (https://github.com/SchlossLab/Lesniak_Severity_XXXX_2022).

585 **Sequence data accession number.** All 16S rRNA gene sequence data and associated
586 metadata are available through the Sequence Read Archive via accession PRJNA787941.

587 **Acknowledgements**

588 Thank you to Sarah Lucas and Sarah Tomkovich for critical discussion in the development
589 and execution of this project. We also thank the University of Michigan Germ-free Mouse
590 Core for assistance with our germfree mice, funded in part by U2CDK110768. This work
591 was supported by several grants from the National Institutes for Health R01GM099514,
592 U19AI090871, U01AI12455, and P30DK034933. Additionally, NAL was supported by the
593 Molecular Mechanisms of Microbial Pathogenesis training grant (NIH T32 AI007528). The
594 funding agencies had no role in study design, data collection and analysis, decision to
595 publish, or preparation of the manuscript.

596 Conceptualization: N.A.L., A.M.S., K.J.F., P.D.S.; Data curation: N.A.L., K.J.F.; Formal analysis:
597 N.A.L., K.J.F., J.L.L., I.L.B.; Investigation: N.A.L., A.M.S., H.S., I.L.B., V.B.Y., P.D.S.; Methodology:
598 N.A.L., A.M.S., K.J.F., J.L.L., H.S., I.L.B., V.B.Y., P.D.S.; Resources: N.A.L., A.M.S., P.D.S.; Software:
599 NAL; Visualization: N.A.L., K.J.F., P.D.S.; Writing - original draft: N.A.L.; Writing - review &
600 editing: N.A.L., A.M.S., K.J.F., J.L.L., H.S., I.L.B., V.B.Y., P.D.S.; Funding acquisition: V.B.Y.;
601 Project administration: P.D.S.; Supervision: P.D.S.

Deleted:Page Break.....

604 **References**

- 605 1. **Kelly CP, LaMont JT.** 2008. *Clostridium difficile*—more difficult than ever. New England
606 Journal of Medicine **359**:1932–1940. doi:[10.1056/nejmra0707500](https://doi.org/10.1056/nejmra0707500).
- 607 2. **McDonald LC, Gerding DN, Johnson S, Bakken JS, Carroll KC, Coffin SE, Dubberke ER,**
608 **Garey KW, Gould CV, Kelly C, Loo V, Sammons JS, Sandora TJ, Wilcox MH.** 2018. Clinical
609 practice guidelines for *Clostridium difficile* infection in adults and children: 2017 update by
610 the infectious diseases society of america (IDSA) and society for healthcare epidemiology of
611 america (SHEA). Clinical Infectious Diseases **66**:e1–e48. doi:[10.1093/cid/cix1085](https://doi.org/10.1093/cid/cix1085).
- 612 3. **Perry DA, Shirley D, Micic D, Patel CP, Putler R, Menon A, Young VB, Rao K.** 2021.
613 External validation and comparison of *Clostridioides difficile* severity scoring systems.
614 Clinical Infectious Diseases. doi:[10.1093/cid/ciab737](https://doi.org/10.1093/cid/ciab737).
- 615 4. **Buffie CG, Bucci V, Stein RR, McKenney PT, Ling L, Gobourne A, No D, Liu H,**
616 **Kinnebrew M, Viale A, Littmann E, Brink MRM van den, Jeng RR, Taur Y, Sander C,**
617 **Cross JR, Toussaint NC, Xavier JB, Pamer EG.** 2014. Precision microbiome reconstitution
618 restores bile acid mediated resistance to *Clostridium difficile*. Nature **517**:205–208.
619 doi:[10.1038/nature13828](https://doi.org/10.1038/nature13828).
- 620 5. **Britton RA, Young VB.** 2014. Role of the intestinal microbiota in resistance to
621 colonization by *Clostridium difficile*. Gastroenterology **146**:1547–1553.
622 doi:[10.1053/j.gastro.2014.01.059](https://doi.org/10.1053/j.gastro.2014.01.059).
- 623 6. **Hryckowian AJ, Treuren WV, Smits SA, Davis NM, Gardner JO, Bouley DM,** Deleted: 5
624 **Sonnenburg JL.** 2018. Microbiota-accessible carbohydrates suppress *Clostridium difficile*

626 infection in a murine model. *Nature Microbiology* **3**:662–669. doi:[10.1038/s41564-018-0150-6](https://doi.org/10.1038/s41564-018-0150-6).

628 **7. Vila AV, Collij V, Sanna S, Sinha T, Imhann F, Bourgonje AR, Mujagic Z, Jonkers DMAE, Masclee AAM, Fu J, Kurilshikov A, Wijmenga C, Zhernakova A, Weersma RK.**
629
630 2020. Impact of commonly used drugs on the composition and metabolic function of the
631 gut microbiota. *Nature Communications* **11**. doi:[10.1038/s41467-019-14177-z](https://doi.org/10.1038/s41467-019-14177-z).

Deleted: 6

632 **8. Abbas A, Zackular JP.** 2020. Microbe-microbe interactions during *Clostridioides difficile*
633 infection. *Current Opinion in Microbiology* **53**:19–25. doi:[10.1016/j.mib.2020.01.016](https://doi.org/10.1016/j.mib.2020.01.016).

Deleted: 7

634 **9. Jenior ML, Leslie JL, Young VB, Schloss PD.** 2017. *Clostridium difficile* colonizes
635 alternative nutrient niches during infection across distinct murine gut microbiomes.
636 *mSystems* **2**. doi:[10.1128/msystems.00063-17](https://doi.org/10.1128/msystems.00063-17).

Deleted: 8

637 **10. Sorg JA, Sonenshein AL.** 2008. Bile salts and glycine as cogerminants for *Clostridium*
638 *difficile* spores. *Journal of Bacteriology* **190**:2505–2512. doi:[10.1128/jb.01765-07](https://doi.org/10.1128/jb.01765-07).

Deleted: 9

639 **11. Thanissery R, Winston JA, Theriot CM.** 2017. Inhibition of spore germination, growth,
640 and toxin activity of clinically relevant *C. difficile* strains by gut microbiota derived
641 secondary bile acids. *Anaerobe* **45**:86–100. doi:[10.1016/j.janaerobe.2017.03.004](https://doi.org/10.1016/j.janaerobe.2017.03.004).

Deleted: 10

642 **12. Aguirre AM, Yalcinkaya N, Wu Q, Swennes A, Tessier ME, Roberts P, Miyajima F,**
643 **Savidge T, Sorg JA.** 2021. Bile acid-independent protection against *Clostridioides difficile*
644 infection. *PLOS Pathogens* **17**:e1010015. doi:[10.1371/journal.ppat.1010015](https://doi.org/10.1371/journal.ppat.1010015).

Deleted: 11

645 **13. Kang JD, Myers CJ, Harris SC, Kakiyama G, Lee I-K, Yun B-S, Matsuzaki K, Furukawa M, Min H-K, Bajaj JS, Zhou H, Hylemon PB.** 2019. Bile acid 7 α -dehydroxylating gut

Deleted: 12

654 bacteria secrete antibiotics that inhibit *Clostridium difficile*: Role of secondary bile acids.

655 Cell Chemical Biology **26**:27–34.e4. doi:[10.1016/j.chembiol.2018.10.003](https://doi.org/10.1016/j.chembiol.2018.10.003).

656 **14. Leslie JL, Jenior ML, Vendrov KC, Standke AK, Barron MR, O'Brien TJ, Unverdorben** Deleted: 13

657 **L, Thaprawat P, Bergin IL, Schloss PD, Young VB.** 2021. Protection from lethal

658 *Clostridioides difficile* infection via intraspecies competition for cogerminant. mBio **12**.

659 doi:[10.1128/mbio.00522-21](https://doi.org/10.1128/mbio.00522-21).

660 **15. Nagao-Kitamoto H, Leslie JL, Kitamoto S, Jin C, Thomsson KA, Gilliland MG, Kuffa** Deleted: 14

661 **P, Goto Y, Jenq RR, Ishii C, Hirayama A, Seekatz AM, Martens EC, Eaton KA, Kao JY,**

662 **Fukuda S, Higgins PDR, Karlsson NG, Young VB, Kamada N.** 2020. Interleukin-22-

663 mediated host glycosylation prevents *Clostridioides difficile* infection by modulating the

664 metabolic activity of the gut microbiota. Nature Medicine **26**:608–617.

665 doi:[10.1038/s41591-020-0764-0](https://doi.org/10.1038/s41591-020-0764-0).

666 **16. Tomkovich S, Stough JMA, Bishop L, Schloss PD.** 2020. The initial gut microbiota and Deleted: 15

667 response to antibiotic perturbation influence *Clostridioides difficile* clearance in mice.

668 mSphere **5**. doi:[10.1128/msphere.00869-20](https://doi.org/10.1128/msphere.00869-20).

669 **17. Nagpal R, Wang S, Woods LCS, Seshie O, Chung ST, Shively CA, Register TC, Craft S,** Deleted: 16

670 **McClain DA, Yadav H.** 2018. Comparative microbiome signatures and short-chain fatty

671 acids in mouse, rat, non-human primate, and human feces. Frontiers in Microbiology **9**.

672 doi:[10.3389/fmich.2018.02897](https://doi.org/10.3389/fmich.2018.02897).

673 **18. Schubert AM, Rogers MAM, Ring C, Mogle J, Petrosino JP, Young VB, Aronoff DM,** Deleted: 17

674 **Schloss PD.** 2014. Microbiome data distinguish patients with *Clostridium difficile* infection

680 and non-*C. difficile*-associated diarrhea from healthy controls. mBio **5**.

681 doi:[10.1128/mbio.01021-14](https://doi.org/10.1128/mbio.01021-14).

682 **19. Gilliland MG, Erb-Downward JR, Bassis CM, Shen MC, Toews GB, Young VB,** Deleted: 18

683 **Huffnagle GB.** 2012. Ecological succession of bacterial communities during
684 conventionalization of germ-free mice. Applied and Environmental Microbiology **78**:2359–
685 2366. doi:[10.1128/aem.05239-11](https://doi.org/10.1128/aem.05239-11).

686 **20. Chen X, Katchar K, Goldsmith JD, Nanthakumar N, Cheknis A, Gerdung DN, Kelly CP.** Deleted: 19

687 2008. A mouse model of *Clostridium difficile*-associated disease. Gastroenterology
688 **135**:1984–1992. doi:[10.1053/j.gastro.2008.09.002](https://doi.org/10.1053/j.gastro.2008.09.002).

689 **21. Schubert AM, Sinani H, Schloss PD.** 2015. Antibiotic-induced alterations of the murine Deleted: 20
690 gut microbiota and subsequent effects on colonization resistance against *Clostridium*
691 *difficile*. mBio **6**. doi:[10.1128/mbio.00974-15](https://doi.org/10.1128/mbio.00974-15).

692 **22. Cowardin CA, Buonomo EL, Saleh MM, Wilson MG, Burgess SL, Kuehne SA, Schwan
C, Eichhoff AM, Koch-Nolte F, Lyras D, Aktories K, Minton NP, Petri WA.** 2016. The
693 binary toxin CDT enhances *Clostridium difficile* virulence by suppressing protective colonic
694 eosinophilia. Nature Microbiology **1**. doi:[10.1038/nmicrobiol.2016.108](https://doi.org/10.1038/nmicrobiol.2016.108).

696 **23. Seekatz AM, Rao K, Santhosh K, Young VB.** 2016. Dynamics of the fecal microbiome in Deleted: 22
697 patients with recurrent and nonrecurrent *Clostridium difficile* infection. Genome Medicine
698 **8**. doi:[10.1186/s13073-016-0298-8](https://doi.org/10.1186/s13073-016-0298-8).

699 **24. Dieterle MG, Putler R, Perry DA, Menon A, Abernathy-Close L, Perlman NS,
Penkevich A, Standke A, Keidan M, Vendrov KC, Bergin IL, Young VB, Rao K.** 2020. Deleted: 23

707 Systemic inflammatory mediators are effective biomarkers for predicting adverse
708 outcomes in *Clostridioides difficile* infection. mBio **11**. doi:[10.1128/mbio.00180-20](https://doi.org/10.1128/mbio.00180-20).

709 **25.** **Lesniak NA, Schubert AM, Sinani H, Schloss PD.** 2021. Clearance of *Clostridioides* Deleted: 24
710 colonization is associated with antibiotic-specific bacterial changes. mSphere **6**.
711 doi:[10.1128/msphere.01238-20](https://doi.org/10.1128/msphere.01238-20).

712 **26.** **Lungulescu OA, Cao W, Gatskevich E, Tlhabano L, Stratidis JG.** 2011. CSI: A severity Deleted: 25
713 index for *Clostridium difficile* infection at the time of admission. Journal of Hospital
714 Infection **79**:151–154. doi:[10.1016/j.jhin.2011.04.017](https://doi.org/10.1016/j.jhin.2011.04.017).

715 **27.** **Zar FA, Bakkanagari SR, Moorthi KMLST, Davis MB.** 2007. A comparison of Deleted: 26
716 vancomycin and metronidazole for the treatment of *Clostridium difficile*-associated
717 diarrhea, stratified by disease severity. Clinical Infectious Diseases **45**:302–307.
718 doi:[10.1086/519265](https://doi.org/10.1086/519265).

719 **28.** **Masi A di, Leboffe L, Politicelli F, Tonon F, Zennaro C, Caterino M, Stano P, Fischer S,** Deleted: 27
720 **Hägele M, Müller M, Kleger A, Papatheodorou P, Nocca G, Arcovito A, Gori A, Ruoppolo**
721 **M, Barth H, Petrosillo N, Ascenzi P, Bella SD.** 2018. Human serum albumin is an essential
722 component of the host defense mechanism against *Clostridium difficile* intoxication. The
723 Journal of Infectious Diseases **218**:1424–1435. doi:[10.1093/infdis/jiy338](https://doi.org/10.1093/infdis/jiy338).

724 **29.** **Abernathy-Close L, Dieterle MG, Vendrov KC, Bergin IL, Rao K, Young VB.** 2020. Deleted: 28
725 Aging dampens the intestinal innate immune response during severe *Clostridioides difficile*
726 infection and is associated with altered cytokine levels and granulocyte mobilization.
727 Infection and Immunity **88**. doi:[10.1128/iai.00960-19](https://doi.org/10.1128/iai.00960-19).

- 733 **[30.](#) Theriot CM, Koumpouras CC, Carlson PE, Bergin II, Aronoff DM, Young VB.** 2011. Deleted: 29
- 734 Cefoperazone-treated mice as an experimental platform to assess differential virulence of
- 735 *Clostridium difficile* strains. Gut Microbes **2**:326–334. doi:[10.4161/gmic.19142](https://doi.org/10.4161/gmic.19142).
- 736 **[31.](#) Goorhuis A, Bakker D, Corver J, Debast SB, Harmanus C, Notermans DW, Bergwerff AA, Dekker FW, Kuijper EJ.** 2008. Emergence of *Clostridium difficile* infection due to a new hypervirulent strain, polymerase chain reaction ribotype 078. Clinical Infectious Diseases **47**:1162–1170. doi:[10.1086/592257](https://doi.org/10.1086/592257).
- 740 **[32.](#) O'Connor JR, Johnson S, Gerding DN.** 2009. *Clostridium difficile* infection caused by the Deleted: 31
- 741 epidemic BI/NAP1/027 strain. Gastroenterology **136**:1913–1924.
- 742 doi:[10.1053/j.gastro.2009.02.073](https://doi.org/10.1053/j.gastro.2009.02.073).
- 743 **[33.](#) Rao K, Micic D, Natarajan M, Winters S, Kiel MJ, Walk ST, Santhosh K, Mogle JA, Galecki AT, LeBar W, Higgins PDR, Young VB, Aronoff DM.** 2015. *Clostridium difficile* Deleted: 32
- 744 ribotype 027: Relationship to age, detectability of toxins A or B in stool with rapid testing,
- 745 severe infection, and mortality. Clinical Infectious Diseases **61**:233–241.
- 746 doi:[10.1093/cid/civ254](https://doi.org/10.1093/cid/civ254).
- 748 **[34.](#) Walk ST, Micic D, Jain R, Lo ES, Trivedi I, Liu EW, Almassalha LM, Ewing SA, Ring C, Galecki AT, Rogers MAM, Washer L, Newton DW, Malani PN, Young VB, Aronoff DM.** Deleted: 33
- 749 2012. *Clostridium difficile* ribotype does not predict severe infection. Clinical Infectious
- 750 Diseases **55**:1661–1668. doi:[10.1093/cid/cis786](https://doi.org/10.1093/cid/cis786).
- 752 **[35.](#) Carlson PE, Walk ST, Bourgis AET, Liu MW, Kopliku F, Lo E, Young VB, Aronoff DM, Hanna PC.** 2013. The relationship between phenotype, ribotype, and clinical disease in Deleted: 34
- 753

760 human *Clostridium difficile* isolates. *Anaerobe* **24**:109–116.

761 doi:[10.1016/j.anaerobe.2013.04.003](https://doi.org/10.1016/j.anaerobe.2013.04.003).

762 **36. Carlson PE, Kaiser AM, McColm SA, Bauer JM, Young VB, Aronoff DM, Hanna PC.** Deleted: 35

763 2015. Variation in germination of *Clostridium difficile* clinical isolates correlates to disease
764 severity. *Anaerobe* **33**:64–70. doi:[10.1016/j.anaerobe.2015.02.003](https://doi.org/10.1016/j.anaerobe.2015.02.003).

765 **37. Saund K, Pirani A, Lacy B, Hanna PC, Snitkin ES.** 2021. Strain variation in Deleted: 36

766 *Clostridioides difficile* toxin activity associated with genomic variation at both PaLoc and
767 non-PaLoc loci. doi:[10.1101/2021.12.08.471880](https://doi.org/10.1101/2021.12.08.471880).

768 **38. He M, Sebaihia M, Lawley TD, Stabler RA, Dawson LF, Martin MJ, Holt KE, Seth-** Deleted: 37

769 **Smith HMB, Quail MA, Rance R, Brooks K, Churcher C, Harris D, Bentley SD, Burrows**
770 **C, Clark L, Corton C, Murray V, Rose G, Thurston S, Tonder A van, Walker D, Wren BW,**
771 **Dougan G, Parkhill J.** 2010. Evolutionary dynamics of *Clostridium difficile* over short and
772 long time scales. *Proceedings of the National Academy of Sciences* **107**:7527–7532.
773 doi:[10.1073/pnas.0914322107](https://doi.org/10.1073/pnas.0914322107).

774 **39. Butt E, Foster JA, Keedwell E, Bell JE, Titball RW, Bhangu A, Michell SL, Sheridan R.** Deleted: 38

775 2013. Derivation and validation of a simple, accurate and robust prediction rule for risk of
776 mortality in patients with *Clostridium difficile* infection. *BMC Infectious Diseases* **13**.
777 doi:[10.1186/1471-2334-13-316](https://doi.org/10.1186/1471-2334-13-316).

778 **40. Beurden YH van, Hensgens MPM, Dekkers OM, Cessie SL, Mulder CJJ,** Deleted: 39

779 **Vandenbroucke-Grauls CMJE.** 2017. External validation of three prediction tools for
780 patients at risk of a complicated course of *Clostridium difficile* infection: Disappointing in an

786 outbreak setting. Infection Control & Hospital Epidemiology **38**:897–905.

787 doi:[10.1017/ice.2017.89](https://doi.org/10.1017/ice.2017.89).

788 **41. Jenior ML, Leslie JL, Young VB, Schloss PD.** 2018. *Clostridium difficile* alters the
789 structure and metabolism of distinct cecal microbiomes during initial infection to promote
790 sustained colonization. mSphere **3**. doi:[10.1128/msphere.00261-18](https://doi.org/10.1128/msphere.00261-18).

Deleted: 40

791 **42. Staley C, Weingarden AR, Khoruts A, Sadowsky MJ.** 2016. Interaction of gut
792 microbiota with bile acid metabolism and its influence on disease states. Applied
793 Microbiology and Biotechnology **101**:47–64. doi:[10.1007/s00253-016-8006-6](https://doi.org/10.1007/s00253-016-8006-6).

Deleted: 41

794 **43. Long SL, Gahan CGM, Joyce SA.** 2017. Interactions between gut bacteria and bile in
795 health and disease. Molecular Aspects of Medicine **56**:54–65.
796 doi:[10.1016/j.mam.2017.06.002](https://doi.org/10.1016/j.mam.2017.06.002).

Deleted: 42

797 **44. Sorg JA, Sonenshein AL.** 2010. Inhibiting the initiation of *Clostridium difficile* spore
798 germination using analogs of chenodeoxycholic acid, a bile acid. Journal of Bacteriology
799 **192**:4983–4990. doi:[10.1128/jb.00610-10](https://doi.org/10.1128/jb.00610-10).

Deleted: 43

800 **45. Dubois T, Tremblay YDN, Hamiot A, Martin-Verstraete I, Deschamps J, Monot M,**
801 **Briandet R, Dupuy B.** 2019. A microbiota-generated bile salt induces biofilm formation in
802 *Clostridium difficile*. npj Biofilms and Microbiomes **5**. doi:[10.1038/s41522-019-0087-4](https://doi.org/10.1038/s41522-019-0087-4).

Deleted: 44

803 **46. Ng KM, Ferreyra JA, Higginbottom SK, Lynch JB, Kashyap PC, Gopinath S, Naidu N,**
804 **Choudhury B, Weimer BC, Monack DM, Sonnenburg JL.** 2013. Microbiota-liberated host
805 sugars facilitate post-antibiotic expansion of enteric pathogens. Nature **502**:96–99.
806 doi:[10.1038/nature12503](https://doi.org/10.1038/nature12503).

Deleted: 45

813 **47. Ferreyra JA, Wu KJ, Hryckowian AJ, Bouley DM, Weimer BC, Sonnenburg JL.** 2014.
814 Gut microbiota-produced succinate promotes *C. difficile* infection after antibiotic treatment
815 or motility disturbance. *Cell Host & Microbe* **16**:770–777. doi:[10.1016/j.chom.2014.11.003](https://doi.org/10.1016/j.chom.2014.11.003).

Deleted: 46

816 **48. Martin-Verstraete I, Peltier J, Dupuy B.** 2016. The regulatory networks that control
817 *Clostridium difficile* toxin synthesis. *Toxins* **8**:153. doi:[10.3390/toxins8050153](https://doi.org/10.3390/toxins8050153).

Deleted: 47

818 **49. Lawley TD, Clare S, Walker AW, Stares MD, Connor TR, Raisen C, Goulding D, Rad-**
819 **R, Schreiber F, Brandt C, Deakin LJ, Pickard DJ, Duncan SH, Flint HJ, Clark TG, Parkhill**
820 **J, Dougan G.** 2012. Targeted restoration of the intestinal microbiota with a simple, defined
821 bacteriotherapy resolves relapsing *Clostridium difficile* disease in mice. *PLoS Pathogens*
822 **8**:e1002995. doi:[10.1371/journal.ppat.1002995](https://doi.org/10.1371/journal.ppat.1002995).

Deleted: 48

823 **50. Reeves AE, Theriot CM, Bergin IL, Huffnagle GB, Schloss PD, Young VB.** 2011. The
824 interplay between microbiome dynamics and pathogen dynamics in a murine model of
825 *Clostridium difficile* infection. *Gut Microbes* **2**:145–158. doi:[10.4161/gmic.2.3.16333](https://doi.org/10.4161/gmic.2.3.16333).

Deleted: 49

826 **51. Battaglioli EJ, Hale VL, Chen J, Jeraldo P, Ruiz-Mojica C, Schmidt BA, Rekdal VM, Till**
827 **LM, Huq L, Smits SA, Moor WI, Jones-Hall Y, Smyrk T, Khanna S, Pardi DS, Grover M,**
828 **Patel R, Chia N, Nelson H, Sonnenburg JL, Farrugia G, Kashyap PC.** 2018. *Clostridioides*
829 *difficile* uses amino acids associated with gut microbial dysbiosis in a subset of patients
830 with diarrhea. *Science Translational Medicine* **10**. doi:[10.1126/scitranslmed.aam7019](https://doi.org/10.1126/scitranslmed.aam7019).

831 **52. Liu X, Mao B, Gu J, Wu J, Cui S, Wang G, Zhao J, Zhang H, Chen W.** 2021. *Blautia* — a
832 new functional genus with potential probiotic properties? *Gut Microbes* **13**,
833 doi:[10.1080/19490976.2021.1875796](https://doi.org/10.1080/19490976.2021.1875796).

Moved (insertion) [1]

Moved (insertion) [2]

Deleted: 50

- §39 [53. Mabrok HB, Klopfleisch R, Ghanem KZ, Clavel T, Blaut M, Loh G.](#) 2011. Lignan
 840 transformation by gut bacteria lowers tumor burden in a gnotobiotic rat model of breast
 841 cancer. *Carcinogenesis* **33**:203–208. doi:[10.1093/carcin/bgr256](https://doi.org/10.1093/carcin/bgr256).
- §42 [54. Kim CC, Healey GR, Kelly WJ, Patchett ML, Jordens Z, Tannock GW, Sims IM, Bell TJ, Hedderley D, Henrissat B, Rosendale DI.](#) 2019. Genomic insights from *Monoglobus pectinilyticus*: A pectin-degrading specialist bacterium in the human colon. *The ISME Journal* **13**:1437–1456. doi:[10.1038/s41396-019-0363-6](https://doi.org/10.1038/s41396-019-0363-6).
- §46 [55. Choi S-H, Kim J-S, Park J-E, Lee KC, Eom MK, Oh BS, Yu SY, Kang SW, Han K-I, Suh MK, Lee DH, Yoon H, Kim B-Y, Lee JH, Lee JH, Lee J-S, Park S-H.](#) 2019. *Anaerotignum faecicola* sp. Nov., isolated from human faeces. *Journal of Microbiology* **57**:1073–1078. doi:[10.1007/s12275-019-9268-3](https://doi.org/10.1007/s12275-019-9268-3).
- §50 [56. Ueki A, Goto K, Ohtaki Y, Kaku N, Ueki K.](#) 2017. Description of *Anaerotignum aminivorans* gen. Nov., sp. Nov., a strictly anaerobic, amino-acid-decomposing bacterium isolated from a methanogenic reactor, and reclassification of *Clostridium propionicum*, *Clostridium neopropionicum* and *Clostridium lactatifermentans* as species of the genus *anaerotignum*. *International Journal of Systematic and Evolutionary Microbiology* **67**:4146–4153. doi:[10.1099/ijsem.0.002268](https://doi.org/10.1099/ijsem.0.002268).
- §56 [57. Stein RR, Bucci V, Toussaint NC, Buffie CG, Rätsch G, Pamer EG, Sander C, Xavier JB.](#) 2013. Ecological modeling from time-series inference: Insight into dynamics and stability of intestinal microbiota. *PLoS Computational Biology* **9**:e1003388. doi:[10.1371/journal.pcbi.1003388](https://doi.org/10.1371/journal.pcbi.1003388).

Deleted: 51

Moved (insertion) [3]

Moved (insertion) [4]

Moved (insertion) [5]

Deleted: 52. Prado SBR do, Minguzzi BT, Hoffmann C, Fabi JP.

Moved up [2]: 2021.

Moved up [3]: 2019.

Moved up [4]: .[¶](#)
56.

Moved up [1]: . 2018.

Moved up [5]: 2017.

Deleted: Modulation of human gut microbiota by dietary fibers from unripe and ripe papayas: Distinct polysaccharide degradation using a colonic in vitro fermentation model. *Food Chemistry* **348**:129071. doi:[10.1016/j.foodchem.2021.129071](https://doi.org/10.1016/j.foodchem.2021.129071).

53. Muthuramalingam K, Singh V, Choi C, Choi SI, Kim YM, Unno T, Cho M.

Deleted: Dietary intervention using (1, 3)/(1, 6)- β -glucan, a fungus-derived soluble prebiotic ameliorates high-fat diet-induced metabolic distress and alters beneficially the gut microbiota in mice model. *European Journal of Nutrition* **59**:2617–2629. doi:[10.1007/s00394-019-02110-5](https://doi.org/10.1007/s00394-019-02110-5).

54. Han S-H, Yi J, Kim J-H, Lee S, Moon H-W. 2019. Composition of gut microbiota in patients with toxigenic *Clostridioides (Clostridium) difficile*: Comparison between subgroups according to clinical criteria and toxin gene load. *PLOS ONE* **14**:e0212626. doi:[10.1371/journal.pone.0212626](https://doi.org/10.1371/journal.pone.0212626).

55. Duncan SH, Louis P, Flint HJ. 2004. Lactate-utilizing bacteria, isolated from human feces, that produce butyrate as a major fermentation product. *Applied and Environmental Microbiology* **70**:5810–5817. doi:[10.1128/aem.70.10.5810-5817.2004](https://doi.org/10.1128/aem.70.10.5810-5817.2004).

Deleted: Ye J, Lv L, Wu W, Li Y, Shi D, Fang D, Guo F, Jiang H, Yan R, Ye W, Li L

Deleted: Butyrate protects mice against methionine-choline-deficient diet-induced non-alcoholic steatohepatitis by improving gut barrier function, attenuating inflammation and reducing endotoxin levels. *Frontiers in Microbiology* **9**. doi:[10.3389/fmicb.2018.01967](https://doi.org/10.3389/fmicb.2018.01967).

57. Walsh CJ, Guinane CM, O'Toole PW, Cotter PD.

Deleted: A profile hidden markov model to investigate the distribution and frequency of LanB-encoding lantibiotic modification genes in the human oral and gut microbiome. *PeerJ* **5**:e3254. doi:[10.7717/peerj.3254](https://doi.org/10.7717/peerj.3254).

58. Sandiford SK. 2018. Current developments in lantibiotic discovery for treating *Clostridium difficile* infection. *Expert Opinion on Drug Discovery* **14**:71–79. doi:[10.1080/17460441.2019.1549032](https://doi.org/10.1080/17460441.2019.1549032).

59

911 **58.** Nakashima T, Fujii K, Seki T, Aoyama M, Azuma A, Kawasome H. 2021. Novel gut
912 microbiota modulator, which markedly increases *Akkermansia muciniphila* occupancy,
913 ameliorates experimental colitis in rats. *Digestive Diseases and Sciences*.
914 doi:[10.1007/s10620-021-07131-x](https://doi.org/10.1007/s10620-021-07131-x).

Deleted: 60

915 **59.** Geerlings S, Kostopoulos I, Vos W de, Belzer C. 2018. *Akkermansia muciniphila* in the
916 human gastrointestinal tract: When, where, and how? *Microorganisms* **6**:75.
917 doi:[10.3390/microorganisms6030075](https://doi.org/10.3390/microorganisms6030075).

Deleted: 61

918 **60.** Deng H, Yang S, Zhang Y, Qian K, Zhang Z, Liu Y, Wang Y, Bai Y, Fan H, Zhao X, Zhi F.
919 2018. *Bacteroides fragilis* prevents *Clostridium difficile* infection in a mouse model by
920 restoring gut barrier and microbiome regulation. *Frontiers in Microbiology* **9**.
921 doi:[10.3389/fmich.2018.02976](https://doi.org/10.3389/fmich.2018.02976).

Deleted: 62

922 **61.** Engevik MA, Engevik AC, Engevik KA, Auchtung JM, Chang-Graham AL, Ruan W,
923 Luna RA, Hyser JM, Spinler JK, Versalovic J. 2020. Mucin-degrading microbes release
924 monosaccharides that chemoattract *Clostridioides difficile* and facilitate colonization of the
925 human intestinal mucus layer. *ACS Infectious Diseases* **7**:1126–1142.
926 doi:[10.1021/acsinfecdis.0c00634](https://doi.org/10.1021/acsinfecdis.0c00634).

Deleted: 63

927 **62.** Reeves AE, Koenigsknecht MJ, Bergin IL, Young VB. 2012. Suppression of *Clostridium*
928 *difficile* in the gastrointestinal tracts of germfree mice inoculated with a murine isolate
929 from the family *Lachnospiraceae*. *Infection and Immunity* **80**:3786–3794.
930 doi:[10.1128/iai.00647-12](https://doi.org/10.1128/iai.00647-12).

Deleted: 64

936 [63. Ma L, Keng J, Cheng M, Pan H, Feng B, Hu Y, Feng T, Yang F.](#) 2021. Gut microbiome
937 and serum metabolome alterations associated with isolated dystonia. *mSphere* **6**.
938 doi:[10.1128/msphere.00283-21](https://doi.org/10.1128/msphere.00283-21).

Deleted: 65

939 [64. Haas KN, Blanchard JL.](#) 2020. Reclassification of the *Clostridium clostridioforme* and
940 *Clostridium sphenoides* clades as *Enterocloster* gen. nov. And *Lacrimispora* gen. nov.,
941 Including reclassification of 15 taxa. *International Journal of Systematic and Evolutionary*
942 *Microbiology* **70**:23–34. doi:[10.1099/ijsem.0.003698](https://doi.org/10.1099/ijsem.0.003698).

Deleted: 66

943 [65. Finegold SM, Song Y, Liu C, Hecht DW, Summanen P, Könönen E, Allen SD.](#) 2005.
944 *Clostridium clostridioforme*: A mixture of three clinically important species. *European*
945 *Journal of Clinical Microbiology & Infectious Diseases* **24**:319–324. doi:[10.1007/s10096-005-1334-6](https://doi.org/10.1007/s10096-005-1334-6).

Deleted: 67

947 [66. Tomkovich S, Taylor A, King J, Colovas J, Bishop L, McBride K, Royzenblat S,](#)
948 [Lesniak NA, Bergin IL, Schloss PD.](#) 2021. An osmotic laxative renders mice susceptible to
949 prolonged *Clostridioides difficile* colonization and hinders clearance. *mSphere* **6**.
950 doi:[10.1128/msphere.00629-21](https://doi.org/10.1128/msphere.00629-21).

Deleted: 68. VanInsberghe D, Elsherbini JA, Varian B, Poutahidis T, Erdman S, Polz MF

951 [67. Keith JW, Dong Q, Sorbara MT, Becattini S, Sia JK, Gjonbalaj M, Seok R, Leiner IM,](#)
952 [Littmann ER, Pamer EG.](#) 2020. Impact of antibiotic-resistant bacteria on immune
953 activation and *Clostridioides difficile* infection in the mouse intestine. *Infection and*
954 *Immunity* **88**. doi:[10.1128/iai.00362-19](https://doi.org/10.1128/iai.00362-19).

Moved down [6]: . 2020.

955 [68. Zackular JP, Moore JL, Jordan AT, Juttukonda LJ, Noto MJ, Nicholson MR, Crews JD,](#)
956 [Semler MW, Zhang Y, Ware LB, Washington MK, Chazin WJ, Caprioli RM, Skaar EP.](#)

Deleted: Diarrhoeal events can trigger long-term *Clostridium difficile* colonization with recurrent blooms. *Nature Microbiology* **5**:642–650. doi:[10.1038/s41564-020-0668-2](https://doi.org/10.1038/s41564-020-0668-2).

69. Garza-González E, Mendoza-Olazarán S, Morfin-Otero R, Ramírez-Fontes A, Rodríguez-Zulueta P, Flores-Treviño S, Bocanegra-Ibarias P, Maldonado-Garza H, Camacho-Ortiz A. 2019. Intestinal microbiome changes in fecal microbiota transplant (FMT) vs. FMT enriched with *Lactobacillus* in the treatment of recurrent *Clostridioides difficile* infection. *Canadian Journal of Gastroenterology and Hepatology* **2019**:1–7. doi:[10.1155/2019/4549298](https://doi.org/10.1155/2019/4549298).

70. Shafiq M, Alturkmani H, Zafar Y, Mittal V, Lodhi H, Ullah W, Brewer J. 2020. Effects of co-infection on the clinical outcomes of *Clostridium difficile* infection. *Gut Pathogens* **12**. doi:[10.1186/s13099-020-00348-7](https://doi.org/10.1186/s13099-020-00348-7). 71

Deleted: 72

982 2016. Dietary zinc alters the microbiota and decreases resistance to *Clostridium difficile*
983 infection. *Nature Medicine* **22**:1330–1334. doi:[10.1038/nm.4174](https://doi.org/10.1038/nm.4174).

984 **69.** Berkell M, Mysara M, Xavier BB, Werkhoven CH van, Monsieurs P, Lammens C, Deleted: 73
985 Ducher A, Vehreschild MJGT, Goossens H, Gunzburg J de, Bonten MJM, Malhotra-
986 Kumar S. 2021. Microbiota-based markers predictive of development of *Clostridioides*
987 *difficile* infection. *Nature Communications* **12**. doi:[10.1038/s41467-021-22302-0](https://doi.org/10.1038/s41467-021-22302-0).

988 **70.** Gardiner BJ, Tai AY, Kotsanas D, Francis MJ, Roberts SA, Ballard SA, Junckerstorff Deleted: 74
989 RK, Korman TM. 2014. Clinical and microbiological characteristics of *Eggerthella lenta*
990 bacteremia. *Journal of Clinical Microbiology* **53**:626–635. doi:[10.1128/jcm.02926-14](https://doi.org/10.1128/jcm.02926-14).

991 **71.** Iljazovic A, Roy U, Gálvez EJC, Lesker TR, Zhao B, Gronow A, Amend L, Will SE, Deleted: 75
992 Hofmann JD, Pils MC, Schmidt-Hohagen K, Neumann-Schaal M, Strowig T. 2020.
993 Perturbation of the gut microbiome by *Prevotella* spp. enhances host susceptibility to
994 mucosal inflammation. *Mucosal Immunology* **14**:113–124. doi:[10.1038/s41385-020-0296-4](https://doi.org/10.1038/s41385-020-0296-4).

996 **72.** Nagalingam NA, Robinson CJ, Bergin IL, Eaton KA, Huffnagle GB, Young VB. 2013. Deleted: 76
997 The effects of intestinal microbial community structure on disease manifestation in IL-
998 10^{-/-} mice infected with *Helicobacter hepaticus*. *Microbiome* **1**. doi:[10.1186/2049-2618-1-15](https://doi.org/10.1186/2049-2618-1-15).

1000 **73.** Abernathy-Close L, Barron MR, George JM, Dieterle MG, Vendrov KC, Bergin IL, Deleted: 77
1001 Young VB. 2021. Intestinal inflammation and altered gut microbiota associated with

1007 inflammatory bowel disease render mice susceptible to *Clostridioides difficile* colonization
1008 and infection. mBio. doi:[10.1128/mbio.02733-20](https://doi.org/10.1128/mbio.02733-20).

1009 **74. Pirofski L-a, Casadevall A.** 2008. The damage-response framework of microbial
1010 pathogenesis and infectious diseases, pp. 135–146. In Advances in experimental medicine
1011 and biology. Springer New York.

Deleted: 78

1012 **75. Casadevall A, Pirofski L-a.** 2014. What is a host? Incorporating the microbiota into the
1013 damage-response framework. Infection and Immunity **83**:2–7. doi:[10.1128/iai.02627-14](https://doi.org/10.1128/iai.02627-14).

Deleted: 79

1014 **76. Lundberg R, Toft MF, Metzdorff SB, Hansen CHF, Licht TR, Bahl MI, Hansen AK,**
1015 2020. Human microbiota-transplanted C57BL/6 mice and offspring display reduced
1016 establishment of key bacteria and reduced immune stimulation compared to mouse
1017 microbiota-transplantation. Scientific Reports **10**. doi:[10.1038/s41598-020-64703-z](https://doi.org/10.1038/s41598-020-64703-z).

Moved (insertion) [6]

1018 **77. Frisbee AL, Saleh MM, Young MK, Leslie JL, Simpson ME, Abhyankar MM, Cowardin**
1019 **CA, Ma JZ, Pramoonjago P, Turner SD, Liou AP, Buonomo EL, Petri WA.** 2019. IL-33
1020 drives group 2 innate lymphoid cell-mediated protection during *Clostridium difficile*
1021 infection. Nature Communications **10**. doi:[10.1038/s41467-019-10733-9](https://doi.org/10.1038/s41467-019-10733-9).

Deleted: 80

1022 **78. Tailford LE, Crost EH, Kavanaugh D, Juge N.** 2015. Mucin glycan foraging in the
1023 human gut microbiome. Frontiers in Genetics **6**. doi:[10.3389/fgene.2015.00081](https://doi.org/10.3389/fgene.2015.00081).

Deleted: 81

1024 **79. Sorg JA, Dineen SS.** 2009. Laboratory maintenance of *Clostridium difficile*. Current
1025 Protocols in Microbiology **12**. doi:[10.1002/9780471729259.mc09a01s12](https://doi.org/10.1002/9780471729259.mc09a01s12).

Deleted: 82

1031 [80](#). Winston JA, Thanissery R, Montgomery SA, Theriot CM. 2016. Cefoperazone-treated
1032 mouse model of clinically-relevant *Clostridium difficile* strain R20291. Journal of Visualized
1033 Experiments. doi:[10.3791/54850](https://doi.org/10.3791/54850).

Deleted: 83

1034 [81](#). Kozich JJ, Westcott SL, Baxter NT, Highlander SK, Schloss PD. 2013. Development of
1035 a dual-index sequencing strategy and curation pipeline for analyzing amplicon sequence
1036 data on the MiSeq illumina sequencing platform. Applied and Environmental Microbiology
1037 **79**:5112–5120. doi:[10.1128/aem.01043-13](https://doi.org/10.1128/aem.01043-13).

Deleted: 84

1038 [82](#). Schloss PD, Westcott SL, Ryabin T, Hall JR, Hartmann M, Hollister EB, Lesniewski
1039 RA, Oakley BB, Parks DH, Robinson CJ, Sahl JW, Stres B, Thallinger GG, Horn DJV,
1040 Weber CF. 2009. Introducing mothur: Open-source, platform-independent, community-
1041 supported software for describing and comparing microbial communities. Applied and
1042 Environmental Microbiology **75**:7537–7541. doi:[10.1128/aem.01541-09](https://doi.org/10.1128/aem.01541-09).

Deleted: 85

1043 [83](#). Wang Q, Garrity GM, Tiedje JM, Cole JR. 2007. Naïve bayesian classifier for rapid
1044 assignment of rRNA sequences into the new bacterial taxonomy. Applied and
1045 Environmental Microbiology **73**:5261–5267. doi:[10.1128/aem.00062-07](https://doi.org/10.1128/aem.00062-07).

Deleted: 86

1046 [84](#). Yue JC, Clayton MK. 2005. A similarity measure based on species proportions.
1047 Communications in Statistics - Theory and Methods **34**:2123–2131. doi:[10.1080/sta-200066418](https://doi.org/10.1080/sta-200066418).

Deleted: 87

1049 [85](#). Segata N, Izard J, Waldron L, Gevers D, Miropolsky L, Garrett WS, Huttenhower C.
1050 2011. Metagenomic biomarker discovery and explanation. Genome Biology **12**:R60.
1051 doi:[10.1186/gb-2011-12-6-r60](https://doi.org/10.1186/gb-2011-12-6-r60).

Deleted: 88

1058 **86. Benjamini Y, Hochberg Y.** 1995. Controlling the false discovery rate: A practical and
1059 powerful approach to multiple testing. *Journal of the Royal Statistical Society: Series B*
1060 (Methodological) **57**:289–300. doi:[10.1111/j.2517-6161.1995.tb02031.x](https://doi.org/10.1111/j.2517-6161.1995.tb02031.x).

Deleted: 89

1061 **87. Topçuoğlu B, Lapp Z, Sovacool K, Snitkin E, Wiens J, Schloss P.** 2021. Mikropml:
1062 User-friendly R package for supervised machine learning pipelines. *Journal of Open Source*
1063 Software **6**:3073. doi:[10.21105/joss.03073](https://doi.org/10.21105/joss.03073).

Deleted: 90

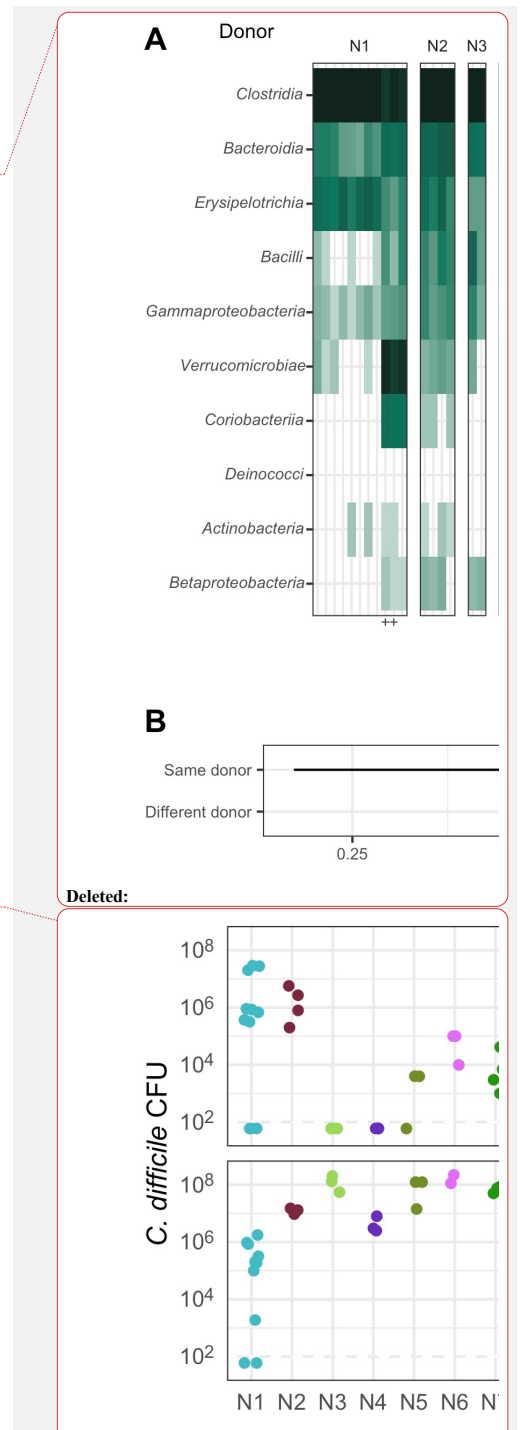
1064 **88. Rawls JF, Mahowald MA, Ley RE, Gordon JI.** 2006. Reciprocal gut microbiota
1065 transplants from zebrafish and mice to germ-free recipients reveal host habitat selection.
1066 *Cell* **127**:423–433. doi:[10.1016/j.cell.2006.08.043](https://doi.org/10.1016/j.cell.2006.08.043).

Deleted: 91

1067

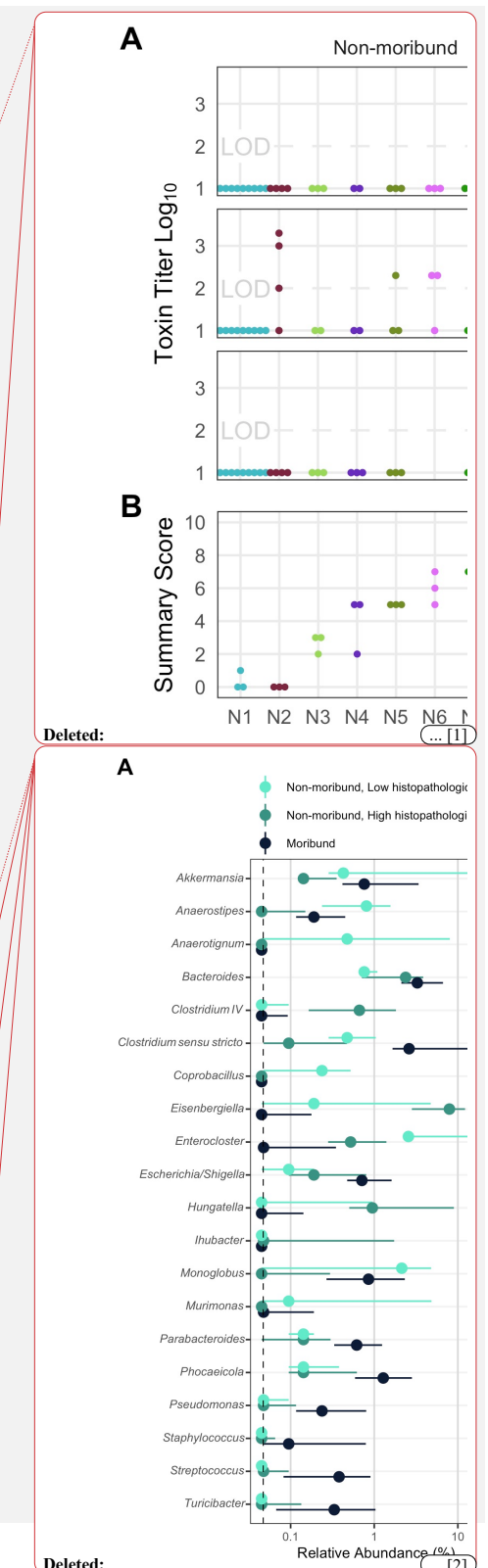
1071 **Figure 1. Human fecal microbial communities established diverse gut bacterial**
 1072 **communities in germ-free mice.** (A) Relative abundances of the 10 most abundant
 1073 bacterial classes observed in the feces of previously germ-free C57Bl/6 mice 14 days post-
 1074 colonization with human fecal samples (i.e., day 0 relative to *C. difficile* challenge). Each
 1075 column of abundances represents an individual mouse. Mice that received the same donor
 1076 feces are grouped together and labeled above with a letter (N for non-moribund mice and
 1077 M for moribund mice) and number (ordered by mean histopathologic score of the donor
 1078 group). + indicates the mice which did not have detectable *C. difficile* CFU (Figure 2). (B)
 1079 Median (points) and interquartile range (lines) of β -diversity (θ_{YC}) between an individual
 1080 mouse and either all others which were inoculated with feces from the same donor or from
 1081 a different donor. The β -diversity among the same donor comparison group was
 1082 significantly less than the β -diversity of either the different donor group or the donor
 1083 community ($P < 0.05$, calculated by Wilcoxon rank sum test).

1084 **Figure 2. All donor groups resulted in *C. difficile* infection but with different**
 1085 **outcomes.** *C. difficile* CFU per gram of stool was measured the day after challenge with 10^3
 1086 *C. difficile* RT027 clinical isolate 431 spores and at the end of the experiment, 10 days post-
 1087 challenge. Each point represents an individual mouse. Mice are grouped by donor and
 1088 labeled by the donor letter (N for non-moribund mice and M for moribund mice) and
 1089 number (ordered by mean histopathologic score of the donor group). Points are colored by
 1090 donor group. Mice from donor groups N1 through N6 succumbed to the infection prior to
 1091 day 10 and were not plated on day 10 post-challenge. LOD = Limit of detection. Deceased-
 1092 indicates mice were deceased at that time point so no sample was available.



1097 **Figure 3. Histopathologic score and toxin activity varied across donor groups.** (A)
 1098 Fecal toxin activity was detected in some mice post *C. difficile* challenge in both moribund
 1099 and non-moribund mice. (B) Cecum scored for histopathologic damage from mice at the
 1100 end of the experiment. Samples were collected for histopathologic scoring on day 10 post-
 1101 challenge for non-moribund mice or the day the mouse succumbed to the infection for the
 1102 moribund group (day 2 or 3 post-challenge). Each point represents an individual mouse.
 1103 Mice are grouped by donor and labeled by the donor letter (N for non-moribund mice and
 1104 M for moribund mice) and number (ordered by mean histopathologic score of the donor
 1105 group). Points are colored by donor group. Mice in group N1 that have a summary score of
 1106 0 are the mice which did not have detectable *C. difficile* CFU (Figure 2). Missing points are
 1107 from mice that had insufficient fecal sample collected for assaying toxin or cecum for
 1108 histopathologic scoring. * indicates significant difference between non-moribund and
 1109 moribund groups of mice by Wilcoxon test ($P < 0.002$). LOD = Limit of detection. -Deceased-
 1110 indicates mice were deceased at that time point so no sample was available.

1111 **Figure 4. Individual fecal bacterial community members of the murine gut associated**
 1112 **with *C. difficile* infection outcomes.** (A and B) Relative abundance of OTUs at the time of
 1113 *C. difficile* challenge (Day 0) that varied significantly by the moribundity and
 1114 histopathologic summary score or detected toxin by LEfSe analysis. Median (points) and
 1115 interquartile range (lines) are plotted. (A) Day 0 relative abundances were compared
 1116 across infection outcome of moribund (colored black) or non-moribund with either a high
 1117 histopathologic score (score greater than the median score of 5, colored green) or a low
 1118 histopathologic summary score (score less than the median score of 5, colored light green).
 1119 (B) Day 0 relative abundances were compared between mice which toxin activity was

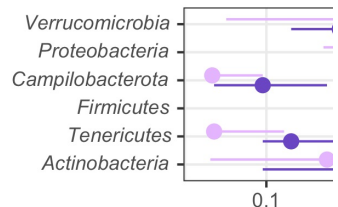


1176 detected (Toxin +, colored dark purple) and which no toxin activity was detected (Toxin -,
 1177 colored light purple). (C) Day 10 bacterial OTU relative abundances correlated with
 1178 histopathologic summary score. Each individual mouse is plotted and colored according to
 1179 their categorization in panel A. Points at the median score of 5 (gray points) were not
 1180 included in panel A. Spearman's correlations were statistically significant after Benjamini-
 1181 Hochberg correction for multiple comparisons. All bacterial groups are ordered by the LDA
 1182 score.* indicates that the bacterial group was unclassified at lower taxonomic classification
 1183 ranks.

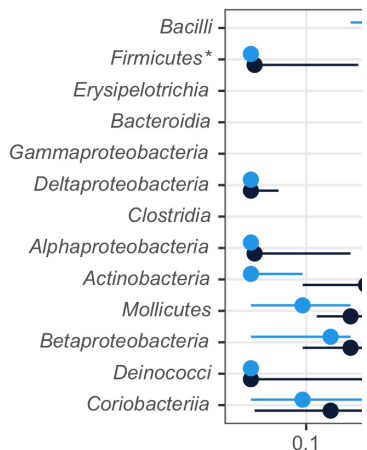
1184 **Figure 5. Fecal bacterial community members of the murine gut at the time of C.**
 1185 **difficile infection predicted outcomes of the infection.** On the day of infection (Day 0),
 1186 bacterial community members grouped by different classification rank were modeled with
 1187 logistic regression to predict the infection outcome. The models used the highest taxonomic
 1188 classification rank without a decrease in performance. Models used all community
 1189 members but plotted are those members with a mean odds ratio not equal to 1. Median
 1190 (solid points) and interquartile range (lines) of the group relative abundance are plotted.
 1191 Bacterial groups are ordered by their odds ratio.* indicates that the bacterial group was
 1192 unclassified at lower taxonomic classification ranks. (A) Bacterial members grouped by
 1193 genus predicted which mice would have toxin activity detected at any point throughout the
 1194 infection (Toxin +, dark purple). (B) Bacterial members grouped by order predicted which
 1195 mice would become moribund (dark blue). (C) Bacterial members grouped by OTU
 1196 predicted if the mice would have a high (score greater than the median score of 5, colored
 1197 dark green) or low (score less than the median score of 5, colored light green)
 1198 histopathologic summary score.

Deleted: Endpoint...ay 10 bacterial OTUs...TU relative abundances correlated with histopathologic summary score. Each individual mouse is plotted (transparent ...nd colored according to their categorization in panel A. Points at the median score of 5 (gray point)...oints) were not included in panel A. Spearman's correlations were statistically significant after Benjamini-Hochberg correction for multiple comparisons. All bacterial groups are ordered alphabetically. (... [3])

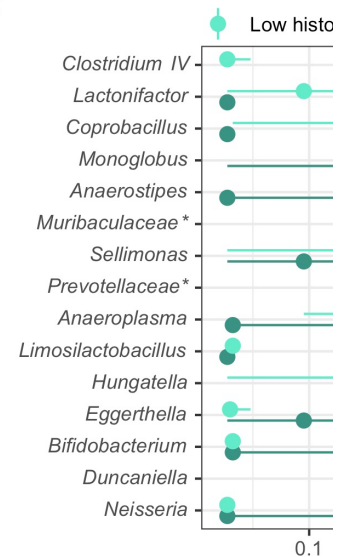
A



B



C



Deleted: (... [4])

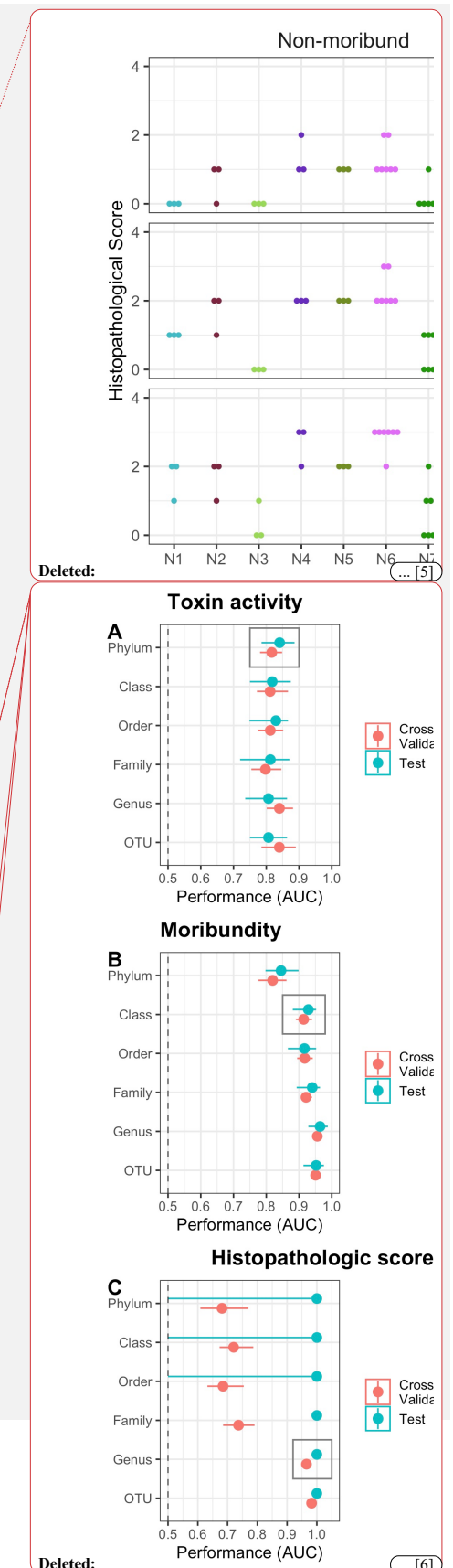
1236 **Figure S1. Toxin detect in mice based on outcome of the infection.** Comparison of the
 1237 distribution of number of either non-moribund or moribund mice which toxin was
 1238 detected in the first three days post infection. Bars are colored by whether toxin was
 1239 detected in stool from the mouse (dark purple) or not (light purple). Moribund mice had
 1240 significantly more mice with toxin detected ($P < 0.008$) by Pearson's Chi-square test.

1241 **Figure S2. Histopathologic score of tissue damage at the endpoint of the infection.**

1242 Tissue collected at the endpoint, either day 10 post-challenge (Non-moribund) or day mice
 1243 succumbed to infection (Moribund), were scored from histopathologic damage. Each point
 1244 represents an individual mouse. Mice (points) are grouped and colored by their human
 1245 fecal community donor. Missing points are from mice that had insufficient sample for
 1246 histopathologic scoring. * indicates significant difference between non-moribund and
 1247 moribund groups of mice by Wilcoxon test ($P < 0.002$).

1248 **Figure S3. Logistic regression models predicted outcomes of the *C. difficile* challenge.**

1249 (A-C) Taxonomic classification rank model performance. Relative abundance at the time of
 1250 *C. difficile* challenge (Day 0) of the bacterial community members grouped by different
 1251 classification rank were modeled with random forest to predict the infection outcome. The
 1252 models used the highest taxonomic classification rank performed as well as the lower
 1253 ranks. Black rectangle highlights classification rank used to model each outcome. For all
 1254 plots, median (large solid points), interquartile range (lines), and individual models (small
 1255 transparent points) are plotted. (A) Toxin production modeled which mice would have
 1256 toxin detected during the experiment. (B) Moribundity modeled which mice would
 1257 succumb to the infection prior to day 10 post-challenge. (C) Histopathologic score modeled



1294 which mice would have a high (score greater than the median score of 5) or low (score less
1295 than the median score of 5) histopathologic summary score.

1296 **Figure S4. Temporal dynamics of OTUs that differed between histopathologic**
1297 **summary score. Relative abundance of OTUs on each day relative to the time of *C. difficile***
1298 **challenge (Day 0) that have a significantly different temporal trend by the histopathologic**
1299 **summary score by LEfSe analysis. Median (points) and interquartile range (lines) are**
1300 **plotted. Points and lines are colored by infection outcome of moribund (colored black) or**
1301 **non-moribund with either a high histopathologic score (score greater than the median**
1302 **score of 5, colored green) or a low histopathologic summary score (score less than the**
1303 **median score of 5, colored light green).**

1304 **Table S1. Demographic information of subjects whose stool samples used to colonize**
1305 **germ-free mice.**

Deleted: (D) Bacterial phyla which affected the performance of predicting detectable toxin activity when permuted. (E) Bacterial classes which affected the performance of predicting moribundity when permuted. (F) Bacterial genera which affected the performance of predicting histopathologic score when permuted.

Page 38: [1] Deleted	Lesniak, Nicholas	4/27/22 4:57:00 PM
Page 38: [1] Deleted	Lesniak, Nicholas	4/27/22 4:57:00 PM
Page 38: [2] Deleted	Lesniak, Nicholas	4/27/22 4:57:00 PM
Page 38: [2] Deleted	Lesniak, Nicholas	4/27/22 4:57:00 PM
Page 38: [2] Deleted	Lesniak, Nicholas	4/27/22 4:57:00 PM
Page 38: [2] Deleted	Lesniak, Nicholas	4/27/22 4:57:00 PM
Page 39: [3] Deleted	Lesniak, Nicholas	4/27/22 4:57:00 PM

Page 39: [3] Deleted	Lesniak, Nicholas	4/27/22 4:57:00 PM
----------------------	-------------------	--------------------

Page 39: [3] Deleted	Lesniak, Nicholas	4/27/22 4:57:00 PM
----------------------	-------------------	--------------------

Page 39: [3] Deleted	Lesniak, Nicholas	4/27/22 4:57:00 PM
----------------------	-------------------	--------------------

Page 39: [3] Deleted	Lesniak, Nicholas	4/27/22 4:57:00 PM
----------------------	-------------------	--------------------

Page 39: [4] Deleted	Lesniak, Nicholas	4/27/22 4:57:00 PM
Page 39: [4] Deleted	Lesniak, Nicholas	4/27/22 4:57:00 PM
Page 39: [4] Deleted	Lesniak, Nicholas	4/27/22 4:57:00 PM
Page 39: [4] Deleted	Lesniak, Nicholas	4/27/22 4:57:00 PM
Page 39: [4] Deleted	Lesniak, Nicholas	4/27/22 4:57:00 PM
Page 39: [4] Deleted	Lesniak, Nicholas	4/27/22 4:57:00 PM
Page 39: [4] Deleted	Lesniak, Nicholas	4/27/22 4:57:00 PM
Page 40: [5] Deleted	Lesniak, Nicholas	4/27/22 4:57:00 PM

Page 40: [6] Deleted	Lesniak, Nicholas	4/27/22 4:57:00 PM
Page 40: [6] Deleted	Lesniak, Nicholas	4/27/22 4:57:00 PM
Page 40: [6] Deleted	Lesniak, Nicholas	4/27/22 4:57:00 PM
Page 40: [6] Deleted	Lesniak, Nicholas	4/27/22 4:57:00 PM